



Published in final edited form as:

*J Phys Chem Lett.* ; 4(21): 3636–3640. doi:10.1021/jz401944q.

## Energy Transfer Observed in Live Cells Using Two-Dimensional Electronic Spectroscopy

Peter D. Dahlberg<sup>1</sup>, Andrew F. Fidler<sup>2</sup>, Justin R. Caram<sup>2</sup>, Phillip D. Long<sup>1</sup>, and Gregory S. Engel<sup>2,\*</sup>

<sup>1</sup>Graduate Program in the Biophysical Sciences, Institute for Biophysical Dynamics, and the James Franck Institute, The University of Chicago, Chicago, IL 60637

<sup>2</sup>Department of Chemistry, Institute for Biophysical Dynamics, and the James Franck Institute, The University of Chicago, Chicago, IL, 60637

### Abstract

Two-dimensional electronic spectroscopy (2DES) elucidates electronic structure and dynamics on a femtosecond time scale and has proven to be an incisive tool for probing congested linear spectra of biological systems. However, samples that scatter light intensely frustrate 2DES analysis, necessitating the use of isolated protein chromophore complexes when studying photosynthetic energy transfer processes. We present a method for conducting 2DES experiments that takes only seconds to acquire thousands of 2DES spectra and permits analysis of highly scattering samples, specifically whole cells of the purple bacterium *Rhodobacter sphaeroides*. These *in vivo* 2DES experiments reveal similar timescales for energy transfer within the antennae complex (light harvesting complex 2, LH2) both in the native photosynthetic membrane environment and in isolated detergent micelles.

### Keywords

Photosynthesis; Ultrafast Dynamics; Nonlinear Spectroscopy

Dynamics in photosynthesis span many orders of magnitude in time and space. Following absorption of a photon, energy migrates from the antennae complex, where the majority of solar photons are absorbed, to the reaction center, where charge separation ensues. These initial energy transfer events occur on timescales ranging from hundreds of femtoseconds to several picoseconds and occur with near unity quantum efficiency under low light conditions.<sup>1-3</sup> Two-dimensional electronic spectroscopy (2DES) can interrogate these initial events in photosynthesis. 2DES produces two-dimensional maps that reveal energetic coupling, energy transfer, and solute-solvent dynamics on a femtosecond timescale.<sup>4-6</sup> A 2DES experiment demands stability in the laser and laboratory conditions throughout data acquisition, which often takes minutes or hours to complete. 2DES also requires a robust sample that produces little scatter and will not degrade during the course of the experiment. However, recently developed lock-in detection schemes for 2DES have mitigated the low scatter restriction.<sup>7-8</sup> Previous work has produced the Gradient Assisted Photon Echo Spectroscopy (GRAPES) apparatus, which is capable of taking a complete 2DES spectrum on each shot of the laser.<sup>9-11</sup> Coupling this capability with advances in CMOS detectors, we

\*Corresponding Author: gselgel@uchicago.edu.

**Supporting Information Available:** A complete list of regression parameters for the decays of B800 are given as well as supporting figures highlighting the excitation spectrum used, LH2 absorbance, 2DES pulse sequence, and the improvement from filtering in the  $\omega_T$  domain. This material is available free of charge via the Internet at <http://pubs.acs.org>.

have built an Ultrafast Video Acquisition GRAPES (UVA GRAPES) apparatus, which can acquire 8192 complete 2DES spectra in less than 3.5 seconds, limited only by the 5 kHz repetition rate of the laser. By filtering in conjugate Fourier domains and fast background subtraction, the technique is relatively immune to scattered light. Thus, UVA GRAPES reduces two experimental difficulties associated with 2DES: long-term stability and signal contamination from scattered photons. These advances allow us to conduct a 2DES experiment in living cells of the purple bacterium *Rhodobacter sphaeroides*. We use this technique to monitor energy transfer in the light harvesting complex two (LH2), the dominant antennae complex of *Rhodobacter sphaeroides*.<sup>12-13</sup>

*In vivo* LH2 is embedded in the plasma membrane and is adjacent to another protein chromophore antennae complex in *Rhodobacter sphaeroides*, light harvesting complex 1 (LH1).<sup>14</sup> During photosynthetic light harvesting, energy is absorbed by LH2 and passed to LH1 and subsequently to the reaction center.<sup>3, 15</sup> LH2 has two characteristic rings of bacteriochlorophyll a known as the B850 and the B800 bands named for their strong absorption peaks at 850 nm and 800 nm respectively, as shown in Supporting Information Figure S1.<sup>16</sup> The 18 B850 bacteriochlorophyll a are strongly coupled,  $\sim 300\text{ cm}^{-1}$ , resulting in their red shifted absorption to 850 nm in contrast to the 9 weakly coupled,  $\sim 20\text{ cm}^{-1}$ , B800 bacteriochlorophyll a that absorb at 800 nm.<sup>17</sup> In addition to the primary absorption of B850 at 850 nm, higher energy excitons exist on the B850 ring; These bands absorb weakly at 800 nm and are known as the B850\* states.<sup>18</sup> The B800 and B850 rings are weakly coupled to each other,  $\sim 20\text{-}50\text{ cm}^{-1}$ .<sup>17, 19</sup> Energy transfer from B800 to B850 has been observed with various techniques in isolated LH2 complexes and found to occur with a lifetime of roughly 700 fs.<sup>3, 20-26</sup>

The foundation of 2DES has been discussed at length elsewhere;<sup>6, 27-32</sup> we therefore limit this discussion to a general description of the experimental procedure and interpretation of the data. 2DES is an ultrafast four-wave mixing experiment that produces an echo signal in a unique phase matched direction for non-collinear geometries. The echo is emitted a rephasing time,  $t$ , after interaction with three ultrafast laser pulses and heterodyne detected using a fourth pulse known as the local oscillator (LO), allowing both the signal field and phase to be measured, as shown in the Supporting Information, Figure S2. Two-dimensional spectra are acquired by systematically scanning the coherence time delay,  $\tau$ , between the first two pulses. After Fourier transforming over the coherence time, filtering, and apodizing, the resulting frequency-frequency map correlates absorption and emission frequencies.<sup>30</sup> The dynamics of energy transfer are obtained by acquiring two-dimensional spectra at various waiting times.

The GRAPES apparatus encodes the coherence time delay spatially across the sample allowing acquisition of entire two-dimensional spectra in a single laser pulse, as shown in Figure 1.<sup>9-11</sup> Here, we present 2DES experiments, each completed in 3.27 seconds, with 8192 waiting times spaced roughly 0.2 fs apart. The GRAPE apparatus only permits the collection of rephasing or non-rephasing signals for a specific scan and all data collected for this manuscript was rephasing only.<sup>33</sup> The supercontinuum pulse used in these experiments was produced via filament generation in argon gas. The output of a 5 kHz Coherent Legend Elite USP regenerative amplifier seeded by a Coherent Micra Ti:Sapphire oscillator was focused into 2.25 meters of argon gas held at 1.3 atm. Filament generation produced a broad spectrum (center = 808 nm FWHM = 70 nm) shown in Supporting Information Figure S1. The resulting spectrum was compressed using Multiphoton Intrapulse Interference Phase Scan (MIIPS) compressor (Biophotonics Solutions Inc.) to  $\sim 15\text{ fs}$  FWHM.<sup>34</sup> Spectra were acquired using a Phantom Miro M high-speed camera from Vision Research. The camera trigger was synchronized to the output of the regenerative amplifier firing at 5 kHz. An optical chopper modulates pulses 1 and 2 at 2.5 kHz resulting in every other laser shot

producing either a complete two-dimensional spectrum or a reference spectrum consisting of only pulses 3 and the LO. The reference spectrum is subtracted from the previous complete two-dimensional spectrum, which was acquired only 200  $\mu\text{s}$  earlier. This fast scatter subtraction minimizes the effect of slow drift in the laser system and improves scatter subtraction capabilities from the conventional scatter subtraction methods outlined by Brixner *et al.*<sup>30</sup> The waiting time was scanned by moving a motorized linear stage (Aerotech ANT130-L) throughout the duration of the experiment at a constant velocity of 75  $\mu\text{m/s}$ . Incident pulse powers for pulses 1-3 were 420 nJ each at the sample. These powers are significantly higher than conventional 2DES experiments because we encode the coherence time delay by focusing to a line ( $\sim 6$  mm by  $\sim 60$   $\mu\text{m}$ ) at the sample rather than to a spot. However, the resulting energy flux of 115  $\mu\text{J/cm}^2$  per pulse is comparable to numerous studies that report similar dynamics and 2DES spectra for LH2; effects due to multi-exciton generation are negligible in this regime.<sup>11, 21, 23, 35</sup> The LO was attenuated by an additional 3 orders of magnitude relative to the other pulses.

LH2 complexes were purified from cultures of *Rhodobacter sphaeroides* in the manner outlined by Frank *et al.*<sup>36</sup> Samples adequate for spectroscopic analysis required two sequential filtrations through a DEAE-Sephacel column followed by elutions with 500-600 mM NaCl. Samples were subsequently concentrated to produce an optical density of roughly 0.3 at 800 nm in a quartz flow cell (Starna Cells Inc.) with a path length of 200  $\mu\text{m}$ . Whole cells were first spun down and frozen and then thawed and diluted with their growth media to achieve an optical density also of 0.3 at 800 nm in the same 200  $\mu\text{m}$  fused quartz flow cell.

The possible contributions from scattered light in the phase matched direction as outlined by Brixner *et al.* are shown in Figure 2A.<sup>30</sup> We isolate the scatter contributions from the signal first by subtraction of the pulse 3 and LO only reference spectrum. Once the reference scatter is removed, we filter in the  $t$  domain and the  $\omega_T$  domain to remove the remaining scatter. The *in vivo* data for all the waiting and rephasing times at  $\tau$  equal to zero after subtraction of the reference is shown in Figure 2B. The signal, the interferogram between the signal field and the LO field spaced  $\sim 3$  ps apart, is well separated in the  $t$  domain from the scattered light produced by pulses spaced 0 to  $\sim 1$  ps apart. Specifically, the interferograms from pulses 1 and 2 interfering with the signal, pulses 1 and 2 interfering with pulse 3, pulses 1 and 2 interfering with themselves, and the signal homodyne are separable from the signal in this domain.<sup>30</sup> However, the signal cannot be isolated from the scatter contributions arising from pulses 1 and 2 interfering with the LO or pulses 1 and 2 interfering with the signal in the  $t$  domain. To filter these scatter contributions from the signal we transform to the  $\omega_T$  domain shown in Figure 2C. These scatter contributions can be removed in this domain because the time difference between interfering electric fields is dependent on  $T$ . As the  $T$  delay stage moves pulses 1 and 2 are delayed relative pulse 3 and the LO. This change in delay causes the electric fields of pulses 1 and 2 to evolve phase relative to pulse 3 and the LO at the optical frequency. This phase evolution is not present in the signal or the scatter contributions, and any dynamics in the signal as a function of  $T$  are of a timescale significantly longer than the optical period,  $\sim 2.7$  fs for 800 nm light. The signal is therefore low-pass filtered in the  $\omega_T$  domain at  $\frac{1}{2}$  the optical frequency and then apodized with a Welch window. Filtering in  $\omega_T$  would not be practical without the single shot capability of UVA GRAPES as  $T$  must be finely sampled to obtain sufficient separation of the optical frequency from the homodyne signals leading to prohibitively long experiments. Waiting times can be recovered for samples with sufficient scatter from pulses 1 and 2, which was the case for all samples discussed in this publication. The waiting time difference between spectra is determined by the slope of  $(E_1+E_2)E_{LO}^*$  at  $\tau$  equal to zero, shown in Figure 2B. The zero of waiting time is located at the intercept of  $(E_1+E_2)E_{LO}$  and the  $E_s E_{LO}^*$  scatter. We found good agreement with the expected values of the waiting time

given the stage settings. Recovered timing data gave a waiting time spacing of  $0.198 \pm 0.005$  fs for a stage setting expected to yield 0.2 fs between spectra.

Two-dimensional spectra of isolated LH2 complexes (*left*) and whole cells (*right*) each at a waiting time of 200 fs are shown in Figure 3, and a larger sampling of 2D spectra from assorted waiting times are shown in Supporting Information Figures S3 and S4. The spectra are normalized to the maximum signal intensity of each experiment separately. The two spectra appear qualitatively very similar despite the fact that the whole cell sample produced significant scatter during acquisition, Supporting Information Figure S5. The two peaks along the diagonal indicate absorption by the B850 and B800 rings from left to right. The cross peaks indicate electronic coupling as well as energy transfer between the two rings in the case of the lower cross peak. The intensity of the B800 band is significantly greater than that of the B850 band, which is the opposite of what would be expected given the linear absorption spectra. This inflated B800 intensity arises from our excitation spectrum only exciting the blue edge of the B850 band while exciting the entirety of the B800 band.

Waiting time traces through the top diagonal (B800) peak for isolated LH2 and whole cells are shown in Figure 4. Energy transfer from B800 to B850 dominates the decay of the B800 diagonal peak and the lifetime corresponds to the energy transfer rate. The decays are analyzed starting at 70 fs to avoid the instrument response function, measured using a solvent blank to be  $\approx 35$  fs FWHM. The decay of isolated LH2 follows a mono-exponential function with a lifetime of  $661 \pm 21$  fs. The whole cell sample shows a similar decay with a lifetime of  $692 \pm 72$  fs, however the whole cell sample shows an additional rapid decay with a lifetime of  $87 \pm 58$  fs. Complete regression parameters are shown in the Supporting Information table S1. The fast decay is likely caused by internal relaxation within the B800 chromophores and may be related to the solvation environment within the lipid membrane.<sup>37</sup> We attribute the long lifetime component to energy transfer from B800 to B850. Our values agree well with known values for the energy transfer rate from B800-B850 of 700 fs.<sup>3, 20-25</sup> This result shows that energy transfer between rings in LH2 is either insensitive to the surrounding lipid environment or that detergent micelles provide a similar enough environment to the true lipid bilayer that effects on energy transfer between rings are negligible. We also observe significant reduction in intensity of the B850 diagonal peak in the whole cell data as shown in Supporting Information table S2 and figure S6. We expect this peak to be diminished in whole cells due to energy transfer from B850 to LH1; however, we would not expect to observe such an effect within 200 fs. The diminished intensity could be indicative of additional intraband relaxation not present in the detergent micelles. Additional studies are needed to produce definitive conclusions regarding the source of differences in the dynamics of the B850 diagonal peak.

UVA GRAPE permits 2DES experiments in whole cells of *Rhodobacter sphaeroides* and shows that energy transfer timescales for LH2 *in vivo* are comparable to timescales for isolated LH2. The technique is largely immune to scatter through fast scatter subtraction and filtering in the  $\omega_T$  domain. Our approach reduces the demands on excitation spectral stability, environmental stability, and sample stability. The ability to achieve high signal to noise 2DES spectra of scattering samples such as whole cells in a matter of seconds will enable of energy transfer events and photoprotection to be studied in real time and in living organisms.

## Supplementary Material

Refer to Web version on PubMed Central for supplementary material.

## Acknowledgments

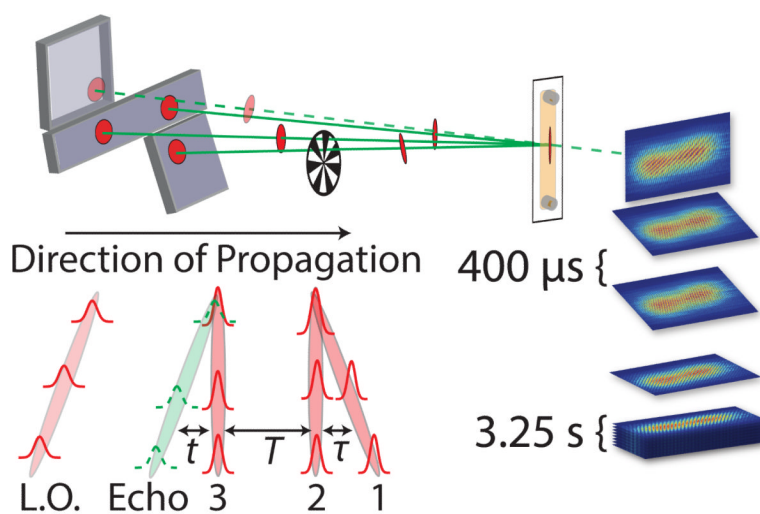
The authors would like to thank NSF MRSEC (Grant No. DMR 08-02054), The Keck Foundation, AFOSR (Grant No. FA9550-09-1-0117), the DARPA QuBE program (N66001-10-1-4060), and DTRA (HDTRA1-10-1-0091) for supporting this work. PDD and JRC acknowledge support from the NSF GRFP. PDD was supported by the Graduate Program in Biophysical Sciences at the University of Chicago (NIH Grant T32 Eb009412). PDL and AFF acknowledge support from the DOE-SCGF program.

## References

- (1). Wraight CA, Clayton RK. The Absolute Quantum Efficiency of Bacteriochlorophyll Photooxidation in Reaction Centres of Rhodospseudomonas Spheroides. *Biochim. Biophys. Acta, Bioenerg.* 1974; 333:246–260.
- (2). Blankenship, RE. *Molecular Mechanisms of Photosynthesis*. Blackwell Science; Oxford ; Malden, MA: 2002. p. 321
- (3). Fleming GR, Grondelle R. v. Femtosecond Spectroscopy of Photosynthetic Light-Harvesting Systems. *Curr. Opin. Struct. Biol.* 1997; 7:738–748. [PubMed: 9345635]
- (4). Schlau Cohen GS, Ishizaki A, Fleming GR. Two-Dimensional Electronic Spectroscopy and Photosynthesis: Fundamentals and Applications to Photosynthetic Light-Harvesting. *Chem. Phys.* 2011; 386:1–22.
- (5). Cho M. Coherent Two-Dimensional Optical Spectroscopy. *Chem. Rev.* 2008; 108:1331–1418. [PubMed: 18363410]
- (6). Jonas DM. Two-Dimensional Femtosecond Spectroscopy. *Annu. Rev. Phys. Chem.* 2003; 54:425–463. [PubMed: 12626736]
- (7). Dostal J, Mancal T, Augulis R, Vacha F, Psencik J, Zigmantas D. Two-Dimensional Electronic Spectroscopy Reveals Ultrafast Energy Diffusion in Chlorosomes. *J. Am. Chem. Soc.* 2012; 134:11611–11617. [PubMed: 22690836]
- (8). Augulis R, Zigmantas D. Two-Dimensional Electronic Spectroscopy with Double Modulation Lock-in Detection: Enhancement of Sensitivity and Noise Resistance. *Opt. Express.* 2011; 19:13126–13133. [PubMed: 21747465]
- (9). Harel E, Fidler AF, Engel GS. Real-Time Mapping of Electronic Structure with Single-Shot Two-Dimensional Electronic Spectroscopy. *Proc. Natl. Acad. Sci. U. S. A.* 2010; 107:16444–16447. [PubMed: 20810917]
- (10). Harel E, Fidler AF, Engel GS. Single-Shot Gradient-Assisted Photon Echo Electronic Spectroscopy. *J. Phys. Chem. A.* 2011; 115:3787–3796. [PubMed: 21090733]
- (11). Harel E, Long PD, Engel GS. Single-Shot Ultrabroadband Two-Dimensional Electronic Spectroscopy of the Light-Harvesting Complex LH2. *Opt. Lett.* 2011; 36:1665–1667. [PubMed: 21540962]
- (12). Cogdell RJ, Gall A, Jurgen K. The Architecture and Function of the Light-Harvesting Apparatus of Purple Bacteria: From Single Molecules to in Vivo Membranes. *Q. Rev. Biophys.* 2006; 39:227–324. [PubMed: 17038210]
- (13). Pullerits T, Chachisvilis M, Jones MR, Hunter CN, Sundström V. Exciton Dynamics in the Light-Harvesting Complexes of *Rhodobacter sphaeroides*. *Chem. Phys. Lett.* 1994; 224:355–365.
- (14). Liu L-N, Scheuring S. Investigation of Photosynthetic Membrane Structure Using Atomic Force Microscopy. *Trends Plant Sci.* 2013; 18:277–286. [PubMed: 23562040]
- (15). Cogdell RJ, Isaacs NW, Howard TD, McLuskey K, Fraser NJ, Prince SM. How Photosynthetic Bacteria Harvest Solar Energy. *J. Bacteriol.* 1999; 181
- (16). McDermott G, Prince SM, Freer AA, Hawthornthwaite-Lawless AM, Papiz MZ, Cogdell RJ, Isaacs NW. Crystal Structure of an Integral Membrane Light-Harvesting Complex from Photosynthetic Bacteria. *Nature.* 1995; 374:517–521.
- (17). Sundström V, Pullerits T, van Grondelle R. Photosynthetic Light-Harvesting: Reconciling Dynamics and Structure of Purple Bacterial LH2 Reveals Function of Photosynthetic Unit. *J. Phys. Chem. B.* 1999; 103:2327–2346.

- (18). Koolhaas MHC, Frese RN, Fowler GJS, Bibby TS, Georgakopoulou S, van der Zwan G, Hunter CN, van Grondelle R. Identification of the Upper Exciton Component of the B850 Bacteriochlorophylls of the LH2 Antenna Complex, Using a B800-Free Mutant of *Rhodobacter sphaeroides*. *Biochemistry*. 1998; 37:4693–4698. [PubMed: 9548732]
- (19). Hildner R, Brinks D, Nieder JB, Cogdell RJ, van Hulst NF. Quantum Coherent Energy Transfer over Varying Pathways in Single Light-Harvesting Complexes. *Science*. 2013; 340:1448–1451. [PubMed: 23788794]
- (20). Herek JL, Fraser NJ, Pullerits T, Martinsson P, Polívka T, Scheer H, Cogdell RJ, Sundström V. B800→B850 Energy Transfer Mechanism in Bacterial LH2 Complexes Investigated by B800 Pigment Exchange. *Biophys. J.* 2000; 78:2590–2596. [PubMed: 10777755]
- (21). Joo T, Jia Y, Yu J-Y, Jonas DM, Fleming GR. Dynamics in Isolated Bacterial Light Harvesting Antenna (LH2) of *Rhodobacter sphaeroides* at Room Temperature. *J. Phys. Chem.* 1996; 100:2399–2409.
- (22). Hess S, Akesson E, Cogdell RJ, Pullerits T, Sundström V. Energy Transfer in Spectrally Inhomogeneous Light-Harvesting Pigment-Protein Complexes of Purple Bacteria. *Biophys. J.* 1995; 69:2211–2225. [PubMed: 8599629]
- (23). Monshouwer R, de Zarate IO, van Mourik F, van Grondelle R. Low-Intensity Pump-Probe Spectroscopy on the B800 to B850 Transfer in the Light Harvesting 2 Complex of *Rhodobacter sphaeroides*. *Chem. Phys. Lett.* 1995; 246:341–346.
- (24). van der Laan H, Schmidt T, Visschers RW, Visscher KJ, van Grondelle R, Völker S. Energy Transfer in the B800–850 Antenna Complex of Purple Bacteria *Rhodobacter sphaeroides*: A Study by Spectral Hole-Burning. *Chem. Phys. Lett.* 1990; 170:231–238.
- (25). Trautman JK, Shreve AP, Violette CA, Frank HA, Owens TG, Albrecht AC. Femtosecond Dynamics of Energy Transfer in B800-850 Light-Harvesting Complexes of *Rhodobacter sphaeroides*. *Proc. Natl. Acad. Sci. USA.* 1990; 87:215–219. [PubMed: 2404276]
- (26). Hess S, Chachisvilis M, Timpmann K, Jones MR, Fowler GJS, Hunter CN, Sundstrom V. Temporally and Spectrally Resolved Subpicosecond Energy Transfer within the Peripheral Antenna Complex (LH2) and from LH2 to the Core Antenna Complex in Photosynthetic Purple Bacteria. *Proc. Natl. Acad. Sci. USA.* 1995; 92:12333–12337. [PubMed: 11607622]
- (27). Mukamel, S. Principles of Nonlinear Optical Spectroscopy. Oxford University Press; New York ; Oxford: 1995.
- (28). Hybl JD, Ferro AA, Jonas DM. Two-Dimensional Fourier Transform Electronic Spectroscopy. *J. Chem. Phys.* 2001; 115:6606–6622.
- (29). Cho M, Vaswani HM, Brixner T, Stenger J, Fleming GR. Exciton Analysis in 2D Electronic Spectroscopy. *J. Phys. Chem. B.* 2005; 109:10542–10556. [PubMed: 16852278]
- (30). Brixner T, Mancal T, Stiopkin IV, Fleming GR. Phase-Stabilized Two-Dimensional Electronic Spectroscopy. *J. Chem. Phys.* 2004; 121:4221–4236. [PubMed: 15332970]
- (31). Cowan ML, Ogilvie JP, Miller RJD. Two-Dimensional Spectroscopy Using Diffractive Optics Based Phased-Locked Photon Echoes. *Chem. Phys. Lett.* 2004; 386:184–189.
- (32). Hybl JD, Albrecht AW, Gallagher Faeder SM, Jonas DM. Two-Dimensional Electronic Spectroscopy. *Chem. Phys. Lett.* 1998; 297:307–313.
- (33). Singh VP, Fidler AF, Rolczynski BS, Engel GS. Independent Phasing of Rephasing and Non-Rephasing 2D Electronic Spectra. *J. Chem. Phys.* 2013; 139:084201. [PubMed: 24006987]
- (34). Lozovoy VV, Pastirk I, Dantus M. Multiphoton Intrapulse Interference. Iv. Ultrashort Laserpulse Spectral Phase Characterization and Compensation. *Opt. Lett.* 2004; 29:775–777. [PubMed: 15072388]
- (35). Fidler AF, Singh VP, Long PD, Dahlberg PD, Engel GS. Timescales of Coherent Dynamics in the Light Harvesting Complex 2 (LH2) Of. *J Phys Chem Lett.* 2013; 4:1404–1409. [PubMed: 23878622]
- (36). Frank HA, Chadwick BW, Jin Oh J, Gust D, Moore TA, Liddell PA, Moore AL, Makings LR, Cogdell RJ. Triplet-Triplet Energy Transfer in B800–850 Light-Harvesting Complexes of Photosynthetic Bacteria and Synthetic Carotenoporphyrin Molecules Investigated by Electron Spin Resonance. *Biochim. Biophys. Acta.* 1987; 892:253–263.

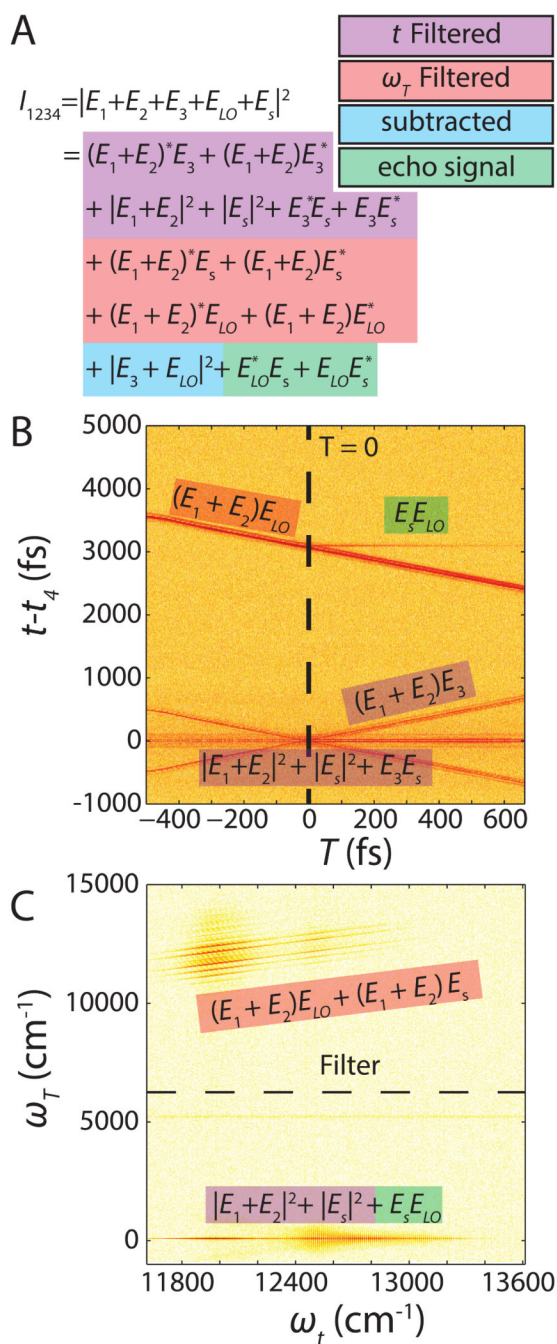
- (37). van Grondelle R, Novoderezhkin VI. Energy Transfer in Photosynthesis: Experimental Insights and Quantitative Models. PCCP. 2006; 8:793–807. [PubMed: 16482320]



**Figure 1.**

The grape mirror produces a slight angle between the wave fronts of pulses 1 and 2 at the focus, which spatially encodes the coherence time and allows for single shot acquisition of a 2DES spectrum. The inset shows the pulse train at the sample. In the extension of GRAPE presented here pulses 1 and 2 are modulated together at 2.5 kHz to produce either a reference composed of pulse 3 and the LO only or a complete 2DES interferogram on every other laser shot. Each laser shot is acquired separately at 5 kHz while the waiting time stage is moving at a constant velocity of  $75 \mu\text{m/s}$ . The data is saved to the camera RAM and is capable of storing 8192 distinct spectra.



**Figure 2.**

(A) Scatter contributions in addition to the desired signal recorded on the camera in a two-dimensional dimensional electronic spectroscopy experiment. The contributions are color coded to reveal how they are eliminated either by subtraction of a reference signal (blue) or filtering in the  $t$  (purple) or  $\omega_T$  (red) domains. (B) A slice at coherence time equal to zero through a waiting time series of 2DES spectra of whole cells. The arcsinh of the data has been computed for display purposes. We can clearly see the separation of the signal from the  $|E_1 + E_2|^2 + |E_s|^2 + E_3 E_s^* + (E_1 + E_2) E_s + c.c.$  (C) Arcsinh of the same data as presented in (B) except a Fourier transform and magnitude have been computed over both domains. The magnitude was computed for display purposes only and is not performed during actual data

analysis. The  $(E_1+E_2)E_{LO}+(E_1+E_2)E_s$  scatter contributions oscillate at the optical frequency in  $T$  allowing their separation from the signal, which varies slowly in  $T$ .

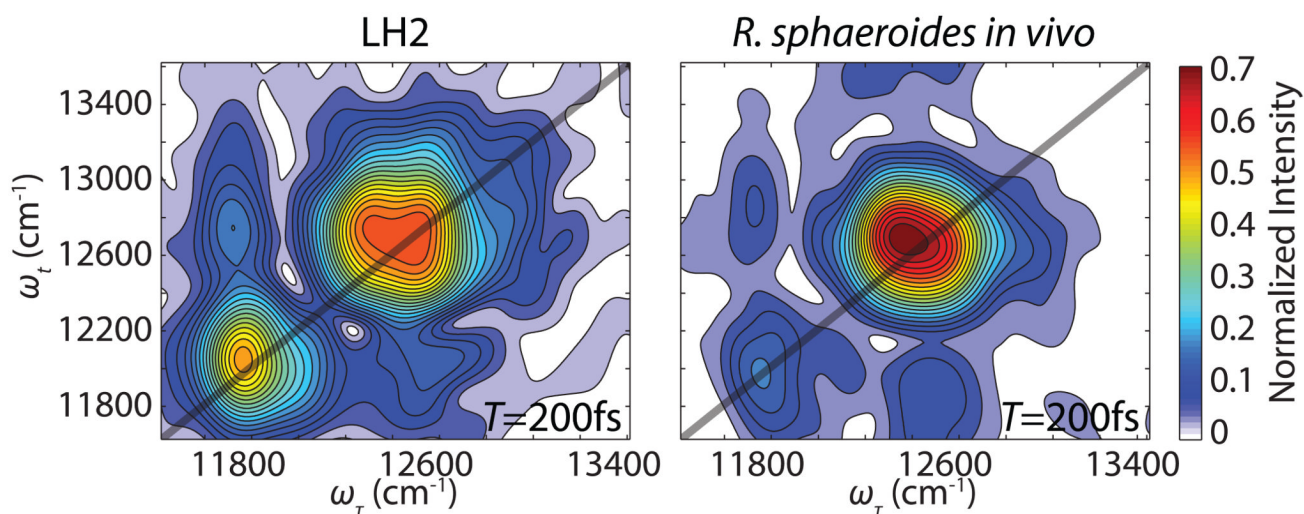


**Figure 3.** Two-dimensional spectra of isolated LH2 (*left*) and whole cells (*right*) both acquired at  $T=200$  fs. The qualitative similarity in structure and signal to noise ratio indicate the ability to remove scatter contributions from the highly scattering cells. The two diagonal peaks correspond to the B850 and B800 absorption features from left to right. The cross peaks indicate energetic coupling and transfer between B800 and B850.

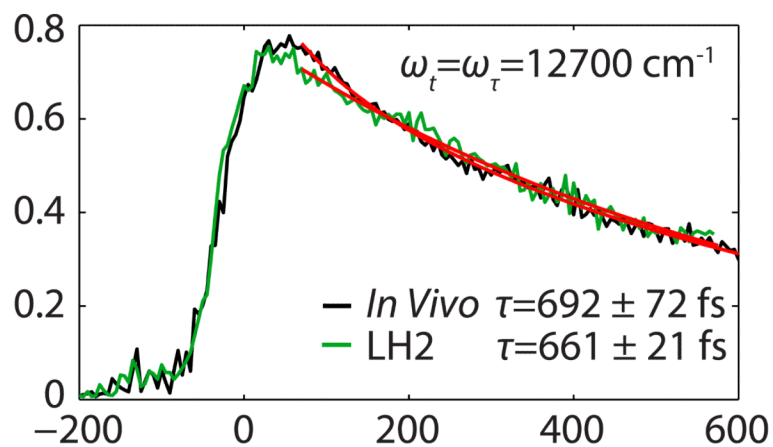


**Figure 4.**

Waiting time traces extracted from the diagonal peak at  $\omega_t = \omega_\tau = 12700$  wavenumbers. The traces were analyzed beginning at  $T = 70$  fs to avoid artifacts from the instrument response function measured to be 35 fs. The *in vivo* trace follows a bi-exponential decay while the isolated LH2 follows a mono-exponential decay. The large amplitude, long lifetime component of the regression parameters is given in the figure and agrees with previous measurements of energy transfer from B800 to B850,  $\sim 700$  fs.